Non-circular Signal DOA Estimation based on Coprime Array MIMO Radar

Fei Zhang (zjzf@just.edu.cn)
Jiangsu University of Science and Technology https://orcid.org/0000-0002-4488-8692
Chuantang Ji
Jiangsu University of Science and Technology
Zijing Zhang
Jiangsu University of Science and Technology
Dayu Yin
Jiangsu University of Science and Technology
Yi Wang
Zhengzhou University School of Architecture

Research

Keywords: Coprime Array, MIMO radar, DOA estimation, MUSIC algorithm

Posted Date: May 10th, 2021

DOI: https://doi.org/10.21203/rs.3.rs-478541/v1

Non-circular signal DOA estimation based on coprime array MIMO radar

Fei Zhang [1], Chuantang Ji [1], Zijing Zhang[1], Dayu Yin[1]

[1] School of Electronic and Information, Jiangsu University of Science and Technology, Zhenjiang 212003, China

Correspondence should be addressed to Fei Zhang; zjzf@just.edu.cn

Abstract: Aiming at the problems of low degree of freedom, small array aperture, phase ambiguity and other problems of traditional coprime array direction of arrival estimation methods, a non-circular signal DOA estimation method based on expanded coprime array MIMO radar is proposed. Firstly, this method combines the coprime array and the MIMO radar to form transmitter and receiver array. Secondly, the array is expanded using the non-circular signal characteristics to reconstruct the received signal matrix. Then the dimensionality reduction is performed. The two-dimensional spectral peak search is converted into an optimization problem, and the optimization of the two-dimensional MUSIC algorithm is reconstructed using constraints, and a cost function is constructed to solve the problem. In addition, using the power series of the noise eigenvalues to correct the noise subspace to further improve the accuracy of the algorithm. Finally, the problem of no phase ambiguity in the method in this article is derived. Simulation experiments show that the method in this article can effectively avoid phase ambiguity, greatly improve the degree of freedom, and expand the array aperture. Compared with the traditional MUSIC algorithm and the mutual prime array MUSIC algorithm, it has better resolution and DOA estimation accuracy.

Keywords: Coprime Array, MIMO radar, DOA estimation, MUSIC algorithm

1 Introduction

Multiple Input Multiple Output (MIMO) technology was introduced into the radar field by Lincoln Laboratory in the United States in 2003 [1], and the concept of MIMO radar was proposed. Compared with traditional radars, MIMO radar has greater advantages in azimuth resolution, array freedom, multi-target parameter estimation, and anti-jamming capabilities, and has been studied and paid attention by many scholars. Direction of Arrival [2-5] (DOA) estimation, as an important research content in array signal processing, has been widely used in sonar, radar, medical and wireless communication fields [6-8]. In recent years, the DOA estimation problem of MIMO radar has been widely concerned and has become a research hotspot.

MIMO radar generally uses a uniform linear array as the transmitter and receiver array, and combines it with the classic high-resolution DOA estimation method to estimate the direction of arrival [9-13]. Classical high-resolution DOA estimation

methods such as Multiple signal classification (MUSIC) method [14-15] or Estimation of signal parameters via rotational invariance techniques (ESPRIT) method [16-17]. However, because uniform linear array is used as the transmitter and receiver array, the spacing of its array elements is generally half a wavelength, and the array aperture is greatly restricted, which affects the performance of MIMO radar angle resolution and multi-target parameter estimation. Therefore, Sparse arrays [18-22] such as nested arrays, coprime arrays and minimum redundant arrays are proposed. Compared with uniform array, Sparse array can use the special arrangement of the array to obtain a larger number of virtual array elements with the same actual number of array elements, and has higher angular resolution and parameter resolution. Reference [23] proposed the structural model of coprime array, two uniform subarrays form coprime array. The number of the subarray elements is M and N, and the distance between the array elements is Nd and Md (d is half the wavelength), And M, N are mutually prime numbers. Reference [24] proposed a coprime array DOA estimation method based on the joint MUSIC algorithm. This method decomposes the coprime array into two uniform subarrays and performs MUSIC estimation separately, and then combines the estimation results of the two subarrays to obtain the final DOA estimation, thereby eliminating the phase ambiguity problem. but this method decomposes the coprime array into Two subarrays lose part of the received data, thereby reducing the DOA estimation performance. Reference [25] proposed a DOA estimation method based on a coprime array. This method expands the coprime array to obtain a virtual array, and introduces spatial smoothing technology to solve the problem that the virtual array is not linear uniform array. but this method will lose the discontinuous information of the array elements, thereby affecting the degree of freedom of DOA estimation. Reference [26-27] respectively proposed the ESPRIT algorithm and the unitary ESPRIT algorithm for the MIMO radar coprime array to jointly estimate the Direction of Departure (DOD) and the Direction of Arrival (DOA). This method divides the coprime array into two uniform sparse subarrays as transmitter and receiver arrays. The coprime array formed by them increases the aperture of the array, thereby improving the performance of DOA estimation. However, the degree of freedom of the above method is limited by the number of elements of the subarray, and additional calculations are required to eliminate the ambiguity problem. Reference [28] proposed DOA estimation method based on the expanded coprime array MIMO radar MUSIC algorithm. This method uses the expanded coprime array as the transmitter and receiver arrays of the MIMO radar to increase the array aperture, and uses the MUSIC algorithm to estimate the DOA, which effectively improves the DOA estimates performance, but this method requires a lot of calculations.

The above literature does not involve DOA estimation methods for non-circular signals. However, there are a large number of non-circular signals in the actual environment [29-30], such as Minimum Shift Keying (MSK) signals, Binary Phase Shift Keying (BPSK) signals and Amplitude Modulation (AM) signals etc. The unique non-circular characteristics of non-circular signals can further expand the virtual array, increase the array aperture, effectively double the dimension of the receiver array, and improve the performance of target parameter estimation and the resolution of multiple

sources. Therefore, based on the literature [28], this article proposes a non-circular signal dimensionality reduction DOA estimation method based on the expanded coprime array MIMO radar (NRC-MIMO MUSIC). This method uses the expanded coprime array MIMO radar model to obtain a larger virtual array when the actual number of array elements is the same. This method first uses the characteristics of non-circular signals to reconstruct the receiver array in the MUSIC algorithm. Then the reconstructed two-dimensional DOA estimation problem is transformed into an optimization problem, and the optimization problem is reconstructed using constraints, and then the Lagrange multiplier method is used to construct the cost function, and the one-dimensional spectral peak search function is obtained. Aiming at the problem of poor accuracy of the method in the environment of low signal-to-noise ratio(SNR) and small number of snapshots, the power series of noise eigenvalues is used to modify the noise subspace to further improve the accuracy of the algorithm. The method proposed in this article uses a coprime array as the transceiver array of the MIMO radar, which greatly increases the array aperture of the virtual array, eliminates the phase ambiguity problem caused by the array element spacing larger than half the wavelength, and significantly improves the DOA estimation performance. Finally, simulation experiments verify the effectiveness of the algorithm. Compared with the classic MUSIC algorithm and the traditional coprime array MUSIC algorithm, the method in this article has better performance in DOA estimation accuracy, successful resolution, and low signal-to-noise ratio (SNR) environments.

2 Preliminaries

The geometric structure of the expanded coprime array MIMO radar is shown in Figure 1. Both the transmitter array and the receiver array are composed of two uniform sparse sub-arrays, the two sub-arrays are expanded side by side, and the last element of subarray 1 is used as the first element of subarray 2. The sparse uniform subarray 1 and subarray 2 together form the expanded coprime array. Subarray 1 contains M array elements, and the distance between each adjacent array element is Nd (where N is the number of array elements and d is half the wavelength). The other sub-array 2 contains N array elements, and the distance between each adjacent array element is Md (where M is the number of array elements and d is half the wavelength). The two numbers M and N are mutually prime, and the distance between adjacent elements of subarray 1 and subarray 2 is greater than half of the wavelength. The formed coprime array contains M+N-1 elements, as shown in Figure 1. The coprime array takes the first element as the reference point, and the position of the element can be expressed as:

$$L_s = \{Mnd | 0 \le n \le N-1\} U \{Nmd | 0 \le m \le M-1\} \tag{1}$$

where $d = \lambda/2$, λ is the wavelength.

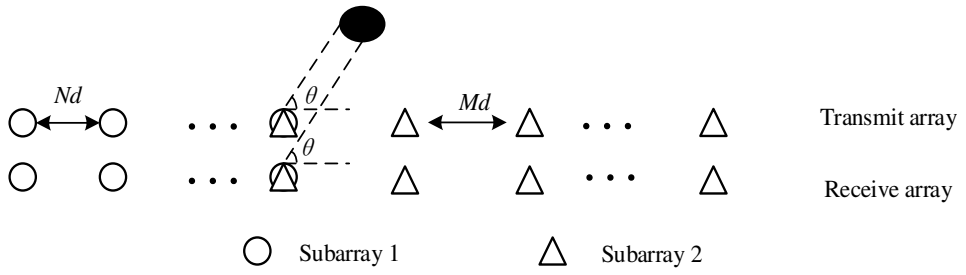

Figure 1. Coprime MIMO radar array geometry

Assume that there are K narrowband far-field uncorrelated signals that are incident on the coprime array at angles [θ_1, θ_2, ..., θ_k], and then the direction vectors of the Kth target of the transmitter array and the receiver array are:

$$a_t(\theta_k)=\left[a_{t1}^T(\theta_k),a_{t2}^T(\theta_k)\right]^T \tag{2}$$

$$a_r(\theta_k)=\left[a_{r1}^T(\theta_k),a_{r2}^T(\theta_k)\right]^T \tag{3}$$

where $a_{t1}(\theta_k)$, $a_{t2}(\theta_k)$ are the direction vectors of the transmitter array subarray 1 and subarray 2 respectively. $a_{r1}(\theta_k)$, $a_{r2}(\theta_k)$ are the direction vectors of the receiver array subarray 1 and subarray 2 respectively. The expressions of the direction vectors of the transmitter sub-array and the receiver subarray are respectively:

$$a_{t1}(\theta_k)=a_{r1}(\theta_k)=\left[1,e^{-j\frac{2\pi Nd\sin(\theta_k)}{\lambda}},\mathrm{L}\ ,e^{-j\frac{2\pi(M-1)Nd\sin(\theta_k)}{\lambda}}\right]^T \tag{4}$$

$$a_{t2}(\theta_k)=a_{r2}(\theta_k)=\left[1,e^{-j\frac{2\pi Md\sin(\theta_k)}{\lambda}},\mathrm{L}\ ,e^{-j\frac{2\pi(N-1)Md\sin(\theta_k)}{\lambda}}\right]^T \tag{5}$$

Therefore, the array flow matrix of the transmitter array and the receiver array are A_t and A_r respectively. It can be expressed as:

$$A_t(\theta)=\left[a_t(\theta_1),a_t(\theta_2),\mathrm{L}\ ,a_t(\theta_K)\right] \tag{6}$$

$$A_r(\theta)=\left[a_r(\theta_1),a_r(\theta_2),\mathrm{L}\ ,a_r(\theta_K)\right] \tag{7}$$

From the above formula (6) and (7), the flow pattern A of the entire virtual array can be obtained as:

$$\begin{aligned}A&=A_r\,\mathrm{o}A_t=\left[a(\theta_1),a(\theta_2),\mathrm{L}\ ,a(\theta_K)\right]\\&=\left[a_r(\theta_1)\otimes a_t(\theta_1),a_r(\theta_2)\otimes a_t(\theta_2),\mathrm{L}\ ,a_r(\theta_K)\otimes a_t(\theta_K)\right]\end{aligned} \tag{8}$$

where $A_r\,\mathrm{o}A_t$ is the Khatri-Rao operator, $a(\theta_k)=a_r(\theta_K)\otimes a_t(\theta_K)$, $\otimes$ represents the Kronecker product. The received signal of the coprime array can be expressed as:

$$x(t)=As(t)+n(t) \tag{9}$$

where $s(t)$ is the source signal vector (non-circular signal vector in this article), $n(t)$ is the noise vector, and A is the array flow matrix.

For the non-circular signal $s(t)$, according to its definition, the non-circular signal

is relative to the circular signal. If the signal has the characteristics of rotation invariance, the signal $s(t)$ is called the circular signal. That is, when $E\{\mathbf{s}(t)\}=\mathbf{0}$, $E\{\mathbf{s}(t)\mathbf{s}^H(t)\}\neq\mathbf{0}$ and $E\{\mathbf{s}(t)\mathbf{s}^T(t)\}=\mathbf{0}$ are established at the same time, $s(t)$ is the circular signal. Conversely, if the signal does not have the characteristics of rotation invariance, then the signal $s(t)$ is called a non-circular signal. That is, when $E\{\mathbf{s}(t)\}=\mathbf{0}$, $E\{\mathbf{s}(t)\mathbf{s}^H(t)\}\neq\mathbf{0}$ and $E\{\mathbf{s}(t)\mathbf{s}^T(t)\}\neq\mathbf{0}$ are established at the same time, $s(t)$ is the non-circular signal. The non-circular signal $s(t)$ can be expressed as:

$$s(t)=\psi s_0(t) \tag{10}$$

where, $\psi=diag\{e_1^{-j\phi_1},e^{-j\phi_2},\mathrm{L}\ ,e^{-j\phi_K}\}$, ϕ_K is the Kth non-circular phase of the non-circular signal, $\boldsymbol{s}_0(t)\in\mathbf{R}^{K\times 1}$.

3 Methods

3.1 Expanded Coprime Array MIMO Radar Non-circular Signal Dimensionality Reduction DOA Estimation Method

From the above formula (9) and (10), the received signal of the coprime array can be expressed as:

$$x(t)=A\psi s_0(t)+n(t) \tag{11}$$

Using the non-circular characteristic of the signal $s(t)$, the array flow matrix can be reconstructed, and the received signal can be reconstructed as:

$$\begin{aligned} y(t)&=\begin{bmatrix}x(t)\\x^*(t)\end{bmatrix}=\begin{bmatrix}A\psi\\A^*\psi^*\end{bmatrix}s_0(t)+\begin{bmatrix}n(t)\\n^*(t)\end{bmatrix}\\&=\boldsymbol{B}s_0(t)+n_0(t)\end{aligned} \tag{12}$$

where, $n_0(t)=\begin{bmatrix}n(t)\\n^*(t)\end{bmatrix}$, $B=\begin{bmatrix}A\Psi\\A^*\Psi^*\end{bmatrix}=\left[\mathbf{b}(\theta_1,\phi_1),\mathbf{b}(\theta_2,\phi_2),\mathrm{L}\ ,\mathbf{b}(\theta_K,\phi_K)\right]^T$, where

$$\mathbf{b}(\theta_K,\phi_K)=\begin{bmatrix}\mathbf{a}(\theta_k)e^{-j\phi_k}\\\mathbf{a}^*(\theta_k)e^{j\phi_k}\end{bmatrix} \tag{13}$$

Then the covariance matrix $R=E[y(t)y^{\mathrm{H}}(t)]$ of the received signal can be obtained from L snapshots. That is

$$\hat{R}=\frac{1}{L}\sum_{l=1}^{L}y(t_l)\,y^H(t_l) \tag{14}$$

Perform eigen decomposition on the covariance matrix A, we can get

$$\hat{R}=E_sD_sE_s^H+E_nD_nE_n^H \tag{15}$$

where, D_s is $K\times K$ diagonal matrix, whose diagonal elements are composed of K larger eigenvalues of the covariance matrix. E_s is the signal subspace, which is the space formed by the eigenvectors corresponding to the K larger eigenvalues of the covariance matrix. D_n is composed of $(M+N\text{-}1)^2\text{-}K$ smaller eigenvalues with smaller diagonal

elements. E_n is the noise subspace, which is the space formed by the eigenvectors corresponding to the $(M+N-1)^2-K$ smaller eigenvalues of the covariance matrix $\hat{R}$. According to the orthogonality between the noise subspace and the direction vector, the following spatial spectrum function is constructed as:

$$P(\theta,\phi)=\frac{1}{b^H(\theta,\phi)E_nE_n^Hb(\theta,\phi)} \tag{16}$$

After reconstructing the receiving matrix from non-circular signals, the spatial spectrum function is a two-dimensional spectral peak search, which is highly complex, and the following dimensionality reduction processing is performed. Firstly, reconstruct the formula (16), then:

$$b(\theta,\phi)=\begin{bmatrix} a(\theta)e^{-j\phi} \\ a^*(\theta)e^{j\phi} \end{bmatrix}=\begin{bmatrix} a(\theta) & 0_{M_1\times 1} \\ 0_{M_1\times 1} & a^*(\theta) \end{bmatrix}\times\begin{bmatrix} e^{-j\phi} \\ e^{j\phi} \end{bmatrix}=P(\theta)e_0(\phi) \tag{17}$$

where,

$$a(\theta)=a_r(\theta)\otimes a_t(\theta) \tag{18}$$

$$P(\theta)=\begin{bmatrix} a(\theta) & 0_{M_1\times 1} \\ 0_{M_1\times 1} & a^*(\theta) \end{bmatrix} \tag{19}$$

$$e_0(\phi)=\begin{bmatrix} e^{-j\phi} \\ e^{j\phi} \end{bmatrix} \tag{20}$$

Define function $V(\theta,\phi)$:

$$V(\theta,\phi)=\frac{1}{P(\theta,\phi)}=b^H(\theta,\phi)E_nE_n^Hb(\theta,\phi) \tag{21}$$

substituting formula (17) into the above formula (21), we can get:

$$\begin{aligned} V(\theta,\phi)&=e_0(\phi)^{\mathrm{H}}P(\theta)^{\mathrm{H}}E_nE_n^HP(\theta)e_0(\phi) \\ &=\mathrm{e}^{-\mathrm{j}\phi}e_0(\phi)^{\mathrm{H}}P(\theta)^{\mathrm{H}}E_nE_n^HP(\theta)e_0(\phi)\mathrm{e}^{\mathrm{j}\phi} \end{aligned} \tag{22}$$

Where, let $q(\phi)=e_0(\phi)\mathrm{e}^{\mathrm{j}\phi}$, $Q(\theta)=P(\theta)^{\mathrm{H}}E_nE_n^HP(\theta)$. Then $V(\theta,\phi)$ can be expressed as:

$$V(\theta,\phi)=q(\phi)^HQ(\theta)q(\phi) \tag{23}$$

where, the above formula (22) is about the problem of quadratic optimization, to find its optimal solution (θ,ϕ). Firstly, increase the constraint of $e^Hq(\phi)=1$ to eliminate the solution of $q(\phi)=0$, so as to obtain the optimal solution (θ,ϕ) of $V(\theta,\phi)$. Use constraints to reconstruct the secondary optimization problem and seek the optimal solution, that is:

$$\min q(\phi)^HQ(\theta)q(\phi)\ \text{ s.t. }\ e^Hq(\phi)=1 \tag{24}$$

The method of solving the optimal solution using the Lagrange multiplier method, Construct the cost function $L(\theta,\phi)$, that is:

$$L(\theta,\phi) = q(\phi)^H Q(\theta) q(\phi) - \lambda\left(e^H q(\phi) - 1\right) \tag{25}$$

where, λ is constant. The partial derivative of formula (25) can be obtained as follows:

$$\frac{\partial L(\theta,\phi)}{\partial q(\phi)} = 2Q(\theta)q(\phi) + \lambda e \tag{26}$$

where, let the above formula (26) be equal to 0, then we can get:

$$q(\phi) = -\frac{\lambda}{2} e Q^{-1}(\theta) \tag{27}$$

Because of the constraint of $e^H q(\phi) = 1$, combined with formula (27), we can get:

$$q(\phi) = \frac{Q^{-1}(\theta)e}{e^{\mathrm{H}} Q^{-1}(\theta)e} \tag{28}$$

Combining formulas (24) and (28) can be obtained:

$$\hat{\theta} = argmin \frac{1}{e^{\mathrm{H}} Q^{-1}(\theta)e} = arg\max e^{\mathrm{H}} Q^{-1}(\theta)e \tag{29}$$

Because of $Q(\theta) = P(\theta)^{\mathrm{H}} E_n E_n^H P(\theta)$, Then the one-dimensional spectral peak search function can be obtained:

$$f(\theta) = e^{\mathrm{H}} Q^{-1}(\theta)e = e^{\mathrm{H}} \left(P(\theta)^{\mathrm{H}} E_n E_n^H P(\theta)\right)^{-1} e \tag{30}$$

In the process of searching for the above-mentioned spectral peaks, the number of snapshots is limited due to the actual situation, which affects the accuracy of the noise subspace E_n, and reduces the DOA estimation performance of the algorithm. For this reason, use the power series of the noise feature to modify the corresponding noise subspace E_n, and the power series of the noise feature:

$$C_n = \left[\lambda_{K+1}^n e_{K+1}, \lambda_{K+2}^n e_{K+2}, \mathrm{L}\ , \lambda_{(M+N-1)^2}^n e_{(M+N-1)^2}\right] \tag{31}$$

where, using formula (31), the above $Q(\theta)$ can be re-expressed as:

$$Q(\theta) = \sum_{i=K+1}^{(M+N-1)^2} \lambda_i^{2n} \left(\left|P(\theta)^H e_i\right|^2\right) \tag{32}$$

Where, substituting formula (32) into the above formula (30), the corrected one-dimensional peak search function can be obtained:

$$f(\theta) = e^{\mathrm{H}} Q^{-1}(\theta)e = e^{\mathrm{H}} \left(\sum_{i=K+1}^{(M+N-1)^2} \lambda_i^{2n} \left(\left|P(\theta)^H e_i\right|^2\right)\right)^{-1} e \tag{33}$$

In summary, the implementation steps of the non-circular signal dimensionality reduction DOA estimation method based on the expanded coprime array MIMO radar proposed in this article are shown in Table 1:

Table 1 The method steps of this article

Step1: The received signal $X(t)$ is constructed from the coprime array model, and the receiving matrix is expanded and reconstructed by formula (10);
Step2: Solve the covariance matrix R by formula (12), and perform eigenvalue decomposition on the covariance matrix to obtain the noise subspace E_n;
Step3: Reconstruct in formula (16) and transform it into a secondary optimization problem;
Step4: Use formulas (24) and (25) to find the optimal solution and get the corresponding $\hat{\theta}$;
Step5: Formula (30) can be obtained by $Q(\theta)$, and $Q(\theta)$ can be corrected by formula (31);
Step6: Finally, the DOA estimated value is obtained from formula (33).

3.2 No phase ambiguity proof

Since the element spacing of the sparse array is greater than half a wavelength, there is a problem of angular ambiguity. But the method in this article adopts the expanded coprime array, which can effectively suppress the phase ambiguity problem. The proof is as follows:

Suppose there is phase ambiguity, that is, there is an ambiguity angle θ_m, which satisfies:

$$a(\hat{\theta}_k) = a(\theta_m) \tag{34}$$

where $\hat{\theta}_k$ is the estimated value of the direction of arrival, and θ_m is the value of the ambiguity angle. From formula (34), we can get:

$$a_r\left(\hat{\theta}_k\right) \otimes a_t\left(\hat{\theta}_k\right) = a_r\left(\theta_m\right) \otimes a_t\left(\theta_m\right) \tag{35}$$

Substituting formulas (2) and (3) into formula (35) above, we can get:

$$\begin{bmatrix} a_{r1}\left(\hat{\theta}_k\right) \\ a_{r2}\left(\hat{\theta}_k\right) \end{bmatrix} \otimes \begin{bmatrix} a_{t1}\left(\hat{\theta}_k\right) \\ a_{t2}\left(\hat{\theta}_k\right) \end{bmatrix} = \begin{bmatrix} a_{r1}\left(\theta_m\right) \\ a_{r2}\left(\theta_m\right) \end{bmatrix} \otimes \begin{bmatrix} a_{t1}\left(\theta_m\right) \\ a_{t2}\left(\theta_m\right) \end{bmatrix} \tag{36}$$

Expand the above formula (36), we can get:

$$\frac{2\pi d_l \sin\hat{\theta}_k}{\lambda} - \frac{2\pi d_l \sin\theta_m}{\lambda} = 2k\pi \tag{37}$$

where, d_l is the element spacing. From the above formula (37), we can get:

$$\begin{cases} \sin\hat{\theta}_k - \sin\theta_m = 2k_1 / M \\ \sin\hat{\theta}_k - \sin\theta_m = 2k_2 / N \end{cases} \tag{38}$$

where, $k_1 \in (-N, N)$, $k_2 \in (-M, M)$. In the coprime array, M and N are integers that are mutually prime numbers. According to theorem 1 of literature [24], it can be known that there is no M and N in formula (36), that is, there is no blur angle θ_m that holds true

in equation (34). That is, it proves that there is no phase ambiguity problem.

4 Results and discussion

In order to verify the effectiveness of the algorithm in this article, the NRC-MIMO MUSIC algorithm in this article is compared with the classic MUSIC algorithm and the traditional coprime array MUSIC algorithm. Define the Root Mean Square Error (RMSE) formula as follows:

$$RMSE = \frac{1}{k}\sum_{1}^{k}\sqrt{\frac{1}{100}\sum_{J=1}^{100}\left(\hat{\theta}_{k,J} - \theta_k\right)^2} \tag{39}$$

where J represents the number of Monte Carlo experiments, $\hat{\theta}_{k,J}$ represents the estimated DOA value of θ_k in the Jth experiment, and θ_k is the true value of the angle.

The proposed algorithm is simulated on MATLAB R2018b software to verify its performance. Set the transmitting array element and the receiving array element to M=3 and N=4 respectively. The number of sources is 2, the target angle is 10° and 20°, the number of snapshots is 100, and the number of Monte Carlo experiments is 100. Figure 2 shows the estimation results of the proposed algorithm for all targets when the SNR=10 dB. It can be seen that the algorithm in this article can accurately estimate the angle of multiple independent targets at the same time.

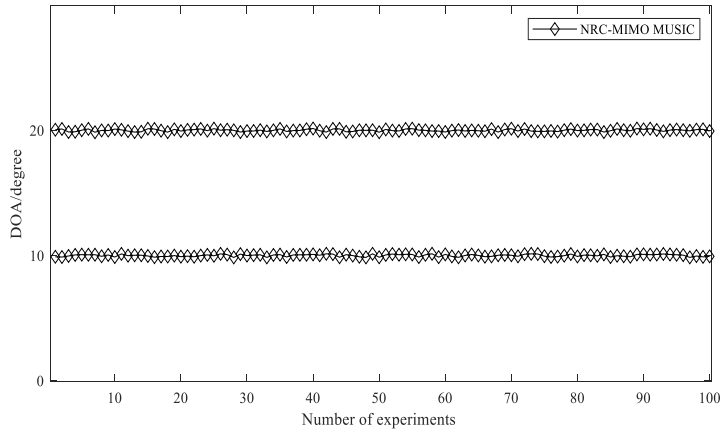

Figure 2. Algorithm estimation performance under SNR=10 dB

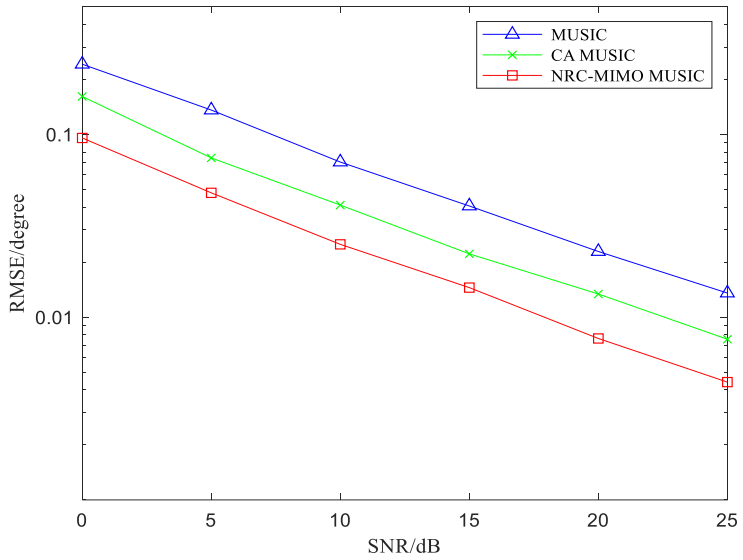

Figure 3. Estimation performance changes under different SNR

Figure 3 shows the DOA of the classic MUSIC algorithm, the traditional coprime array MUSIC algorithm, and the expanded coprime array MIMO radar non-circular signal dimensionality reduction MUSIC algorithm under the condition of 100 snapshots under different SNB Estimated performance. It can be seen from Figure 3 that with the gradual improvement of the signal-to-noise ratio of the three algorithms, the root mean square error RMSE is all getting smaller, and the DOA estimation performance is improved. In addition, it can be seen from the above figure that the algorithm proposed in this article is better than the other two algorithms, and the DOA estimation performance is better. It can also be seen that the relatively prime array can significantly improve the DOA estimation performance compared to the uniform linear array.

Figure 4 shows the classic MUSIC algorithm, the traditional coprime array MUSIC algorithm, and the expanded coprime array MIMO radar non-circular signal dimensionality reduction MUSIC algorithm under 100 effective computer simulation experiments, the target detection success rate varies with the SNR. Target detection success rate, that is, the ratio of the number of successful DOA estimates to the number of trials. When $\left|\hat{\theta}_K\text{-}\theta_K\right|<1$ (where $\hat{\theta}_k$ is the estimated value of DOA and θ_k is the actual value), it is deemed to be a successful estimate of DOA. It can be seen from Figure 4 that the success rate of the three algorithms increases as the SNR increases. When the SNR is equal to 10dB, the success rates of the three algorithms all reach 100%. But when the SNR is less than 10dB, the success rate of this algorithm is better than the other two algorithms. In the case of low SNR, it still maintains a high success rate. This shows that the algorithm in this article is still applicable under the condition of low SNR.

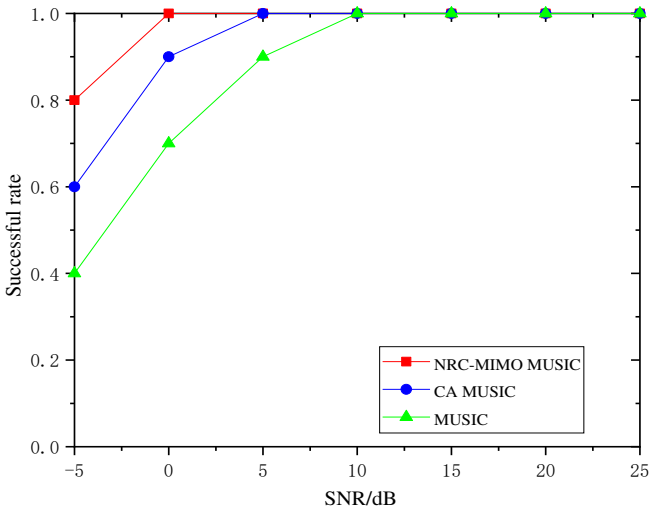

Figure 4. The target detection success rate varies with SNR

Table 2. RMSE value under different SNR

SNR/dB	Classic MUSIC algorithm	Coprime Array MUSIC Algorithm	NRC-MIMO MUSIC Algorithm
0	0.2419	0.1611	0.0955
5	0.1358	0.0742	0.0478
10	0.0705	0.0410	0.0250
15	0.0405	0.0221	0.0145
20	0.0228	0.0133	0.0076
25	0.0135	0.0075	0.0044

Table 2 shows the specific values of the RMSE of the classic MUSIC algorithm, the traditional coprime array MUSIC algorithm, and the expanded coprime array MIMO non-circular signal dimensionality reduction MUSIC algorithm under different SNR. It can be seen from Table 2 that as the SNR increases, the estimation performance of the three algorithms gradually improves. However, the algorithm proposed in this article is better than the other two algorithms under different SNR, and the estimation accuracy is higher. When the SNR is 15dB, the estimation performance of the algorithm proposed in this article can be equivalent to that of the classic MUSIC when the SNR is 25dB. When the SNR=10dB, the RMSE of the algorithm in this article is reduced by about 64% compared to the classic MUSIC algorithm, and about 39% compared with the traditional coprime array MUSIC algorithm. The RMSE of the traditional coprime array MUSIC algorithm is reduced by about 41% Compared with the classic MUSIC algorithm. Therefore, it can be seen that compared to the other two algorithms, the estimation accuracy of the algorithm in this article is higher, and the coprime array can significantly improve the DOA estimation accuracy of the algorithm compared with the uniform linear array.

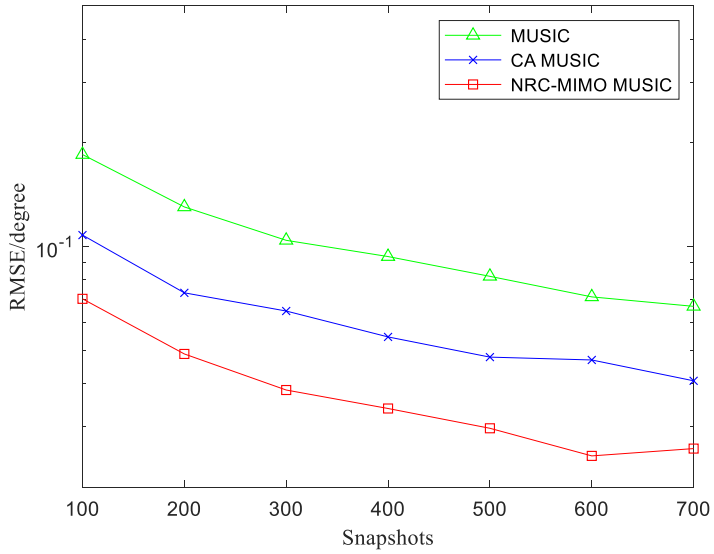

Figure 5. Estimated performance changes under different snapshots

Figure 5 shows the variation of the RMSE of the classic MUSIC algorithm, the traditional coprime array MUSIC algorithm, and the expanded coprime array MIMO radar non-circular signal dimensionality reduction MUSIC algorithm under different snapshots. It can be seen from Figure 5 that as the number of snapshots increases, the RMSE of the three algorithms gradually decreases, and the estimation performance gradually improves. Among them, the classic MUSIC algorithm has the worst angle estimation performance, and the expanded coprime array MIMO radar non-circular signal dimensionality reduction MUSIC algorithm has the best angle estimation performance and is more stable. The algorithm in this article still has good estimation performance when the number of snapshots is low.

Figure 6 shows the classic MUSIC algorithm, the traditional coprime array MUSIC algorithm, and the expanded coprime array MIMO radar non-circular signal dimensionality reduction MUSIC algorithm under 100 effective computer simulation experiments, the target detection success rate varies with the snapshots. It can be seen from Figure 6 that the success rate of the three algorithms increases as the number of snapshots increases. When the number of snapshots is equal to 300, the target detection success rate of the algorithm proposed in this article is almost 100%, and when the number of snapshots is large enough, the target detection success rate of all algorithms can reach 100%. In the case of the same number of snapshots, the algorithm proposed in this article has a higher target detection success rate than the other two algorithms. In the case of a lower number of snapshots, the target detection success rate of the algorithm proposed in this article is significantly higher than that of the classic MUSIC algorithm and traditional coprime array MUSIC algorithm.

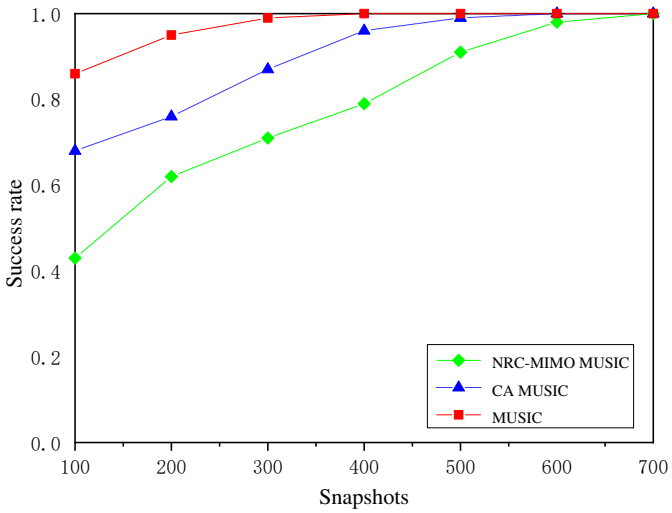

Figure 6. The success rate of target detection varies with the number of snapshots

Table 3. RMSE values under different snapshots

Snapshots	Classic MUSIC algorithm	Coprime Array MUSIC Algorithm	NRC-MIMO MUSIC Algorithm
100	0.1850	0.1079	0.0704
200	0.1303	0.0733	0.0487
300	0.1042	0.0649	0.0382
400	0.0934	0.0546	0.0338
500	0.0819	0.0477	0.0296
600	0.0713	0.0468	0.0246
700	0.0670	0.0407	0.0258

Table 3 shows the specific values of the RMSE of the classic MUSIC algorithm, the traditional coprime array MUSIC algorithm, and the expanded coprime array MIMO non-circular signal dimensionality reduction MUSIC algorithm under different snapshots. It can be seen from Table 3 that, when the number of snapshots is low, the angle estimation accuracy of the classic MUSIC algorithm is the lowest, and the angle estimation accuracy of the algorithm proposed in this article is the highest. As the number of snapshots increases, the RMSE of the classic MUSIC algorithm, the traditional coprime array MUSIC algorithm, and the expanded coprime array MIMO non-circular signal dimensionality reduction MUSIC algorithm gradually decreases, and the accuracy of the algorithm is gradually improved. Among them, the angle estimation accuracy of the algorithm proposed in this article is the highest, and the angle estimation accuracy of the classic MUSIC algorithm is the lowest. In the case of 100 snapshots, the RMSE of the proposed algorithm is about 62% lower than that of the classic MUSIC algorithm, and the RMSE of the traditional coprime array MUSIC algorithm is about 41% lower than that of the classic MUSIC algorithm.

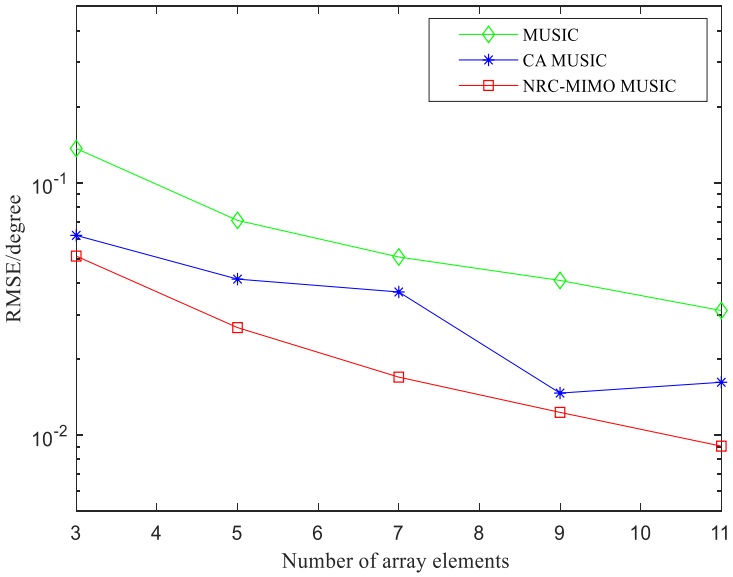

Figure 7. Relationship between the estimation accuracy and the number of array elements

Figure 7 shows the variation of the RMSE of the classic MUSIC algorithm, the traditional coprime array MUSIC algorithm, and the expanded coprime array MIMO radar non-circular signal dimensionality reduction MUSIC algorithm under different the number of array elements. Set the number of transmitting array elements to 4, and the number of receiving array elements to 3, 5, 7, 9, and 11. The number of sources is 2, the target angle is 10° and 20°, the number of snapshots is 100, and the number of Monte Carlo experiments is 100. The experiment parameters are simulated by MATLAB, and RMSE of the three algorithms decreases with the increase of the number of elements, and the accuracy of angle estimation is improved. Among them, the classic MUSIC algorithm has the lowest angle estimation accuracy, and the algorithm proposed in this article has the highest accuracy. In the case of a small number of transmitted array elements, the algorithm proposed in this article has higher estimation accuracy than the other two algorithms.

Table 4. RMSE values under different numbers of array elements

Number of array elements	Classic MUSIC algorithm	Coprime Array MUSIC Algorithm	NRC-MIMO MUSIC Algorithm
3	0.1364	0.0617	0.0511
5	0.0708	0.0414	0.0266
7	0.050	0.0368	0.0169
9	0.040	0.0146	0.0122
11	0.031	0.0161	0.0090

Table 4 shows the specific values of the RMSE of the classic MUSIC algorithm, the traditional coprime array MUSIC algorithm, and the expanded coprime array MIMO non-circular signal dimensionality reduction MUSIC algorithm under different the number of array elements. It can be seen from Table 4 that when the number of array elements is small, the angle estimation accuracy of the classic MUSIC algorithm is the

lowest, and the angle estimation accuracy of the expanded coprime array MIMO non-circular signal dimensionality reduction MUSIC algorithm is the highest. When the number of array elements is 3, the RMSE of the proposed algorithm is about 62% lower than that of the classic MUSIC, and the RMSE of the traditional coprime array MUSIC algorithm is about 54% lower than that of the classic MUSIC algorithm. As the number of array elements increases, the accuracy of each algorithm is gradually improved. The angle estimation accuracy of the algorithm proposed in this article is the highest, and the angle estimation accuracy of the classic MUSIC algorithm is the lowest.

Under the expanded coprime array MIMO radar signal model, set the number of snapshots to 100, the number of sources to 2, the target angle to 10° and 20°, the number of receiving array elements N remains unchanged, and the number of transmitting array elements M to 3, 4, 7. Carry out 100 Monte Carlo experiments, get the RMSE graph of angle measurement accuracy with SNR under different number of transmitting array elements. It can be seen from Figure 8 that in the case of three groups of different transmitting array elements, the algorithms proposed in this paper all increase as the SNR increases, and the accuracy of angle measurement estimation becomes higher. When the number of transmitting array elements is 3, the measurement accuracy is the lowest, and when the number of transmitting array elements is 7, the angle measurement estimation accuracy is the highest.

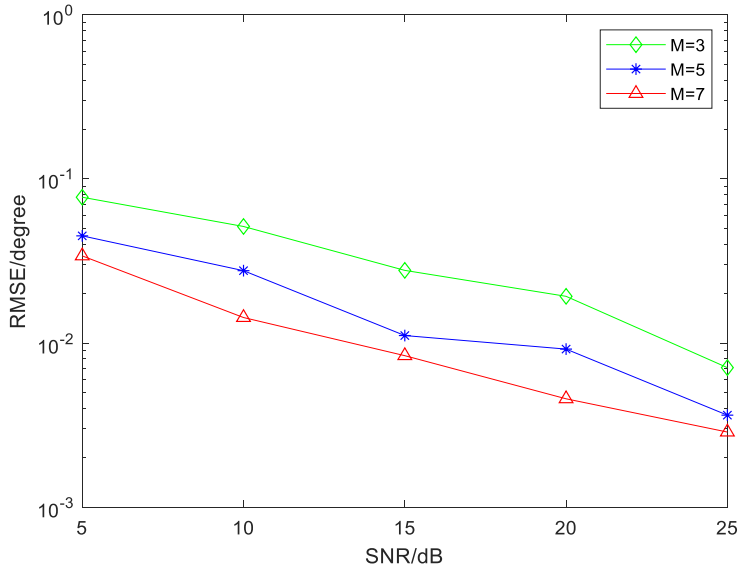

Figure 8. Performance comparison of algorithms with different numbers of transmitting array elements

Table 5 shows the specific values of the root mean square error (RMSE) of the algorithm proposed in this paper with the change of the SNR under different the number of transmitting array elements. It can be seen from Table 5 that when the SNR is low, the angle estimation accuracy is the lowest when the number of transmission elements is 3. The angle estimation accuracy is the highest when the number of transmission elements is 7. When the SNR is 5dB, the RMSE of the transmitting array element M=5 is about 45% lower than the RMSE of M=3. The RMSE of the transmitting array

element M=7 is about 60% lower than the RMSE of M=3. As the signal-to-noise ratio (SNR) increases, the accuracy of the algorithm is gradually improved. Among them, the angle estimation accuracy of the transmitting array element number 3 is the lowest, and the angle estimation accuracy of the transmitting array element number 7 is the highest.

Table 5. RMSE values under different transmitting array elements M and SNR

SNR	M=3	M=5	M=7
5	0.1247	0.0681	0.0493
10	0.0598	0.0414	0.0247
15	0.0427	0.0205	0.0140
20	0.0247	0.0135	0.0105
25	0.0109	0.0066	0.0058

5 Conclusion

In order to solve the problems of low degree of freedom, small array aperture, and phase ambiguity of traditional coprime array direction of arrival estimation methods, this paper proposes a non-circular signal DOA estimation method based on expanded coprime array MIMO radar. This article first combines the expanded coprime array with the MIMO radar to expand the array aperture, improve the DOA estimation performance and increase the degree of freedom. And by introducing non-circular signals, the array aperture is further increased. Then use the idea of dimensionality reduction to reduce the dimensionality of the two-dimensional MUSIC algorithm to reduce the complexity of the algorithm. The power series of noise eigenvalues is used to correct the noise subspace, which further improves the accuracy of the algorithm. Finally, the effectiveness of the algorithm is verified by simulation experiments. Compared with the classic MUSIC algorithm and the traditional MUSIC algorithm, the algorithm in this paper can better improve the DOA estimation accuracy and successful resolution. And it still maintains superior performance under SNR.

Abbreviations:

MIMO: Multiple Input Multiple Output; DOA: Direction of arrival; MUSIC: Multiple signal classification algorithm; SNR: Signal-to-noise ratio; RMSE: Root mean square error; CA: Coprime Array; NRC-MIMO MUSIC: Non-circular signal dimensionality reduction DOA estimation method based on the expanded coprime array MIMO radar

Acknowledgments:

The authors would like to thank Aisuo Jin for his academic support, and I can finish the thesis successfully.

Authors' contributions:

All authors have contributed towards this work as well as in compilation of this manuscript. The author(s) read and approved the final manuscript.

Funding Statement:

This work was supported by the National Natural Science Foundation of China under Grant No.61801170 and 61801435, and Jiangsu Overseas Visiting Scholar Program for University Prominent Yong & Middle-aged Teachers and Presidents.

Availability of data and materials:

All data generated or analyzed during this study are included in this published article.

Declarations

Competing interests:

The authors declare that they have no conflicts of interest.

Ethics approval and consent to participate:

Not applicable.

Consent for publication:

Not applicable.

References

1. D. W. Bliss, K. W. Forsythe. Multiple-input multiple-output (MIMO) radar and imaging: degrees of freedom and resolution[C]// Signals, Systems and Computers, 2003. Conference Record of the Thirty-Seventh Asilomar Conference on. 2003.
2. F. Mendoza-Montoya, D. H. Covarrubias-Rosales, C. A. Lopez-Miranda. DOA Estimation in Mobile Communications System using Subspace Tracking Methods[J]. Latin America transactions, 2008, 6(2):123-129.
3. J. Y. Liu, Y. L. Lu, Y. M. Zhang, et al. Fractional difference co-array perspective for wideband signal DOA estimation[J]. EURASIP J. Adv. Signal Process. 2016, 133 (2016).
4. P. Gupta, K. Aditya, A. Datta. Comparison of conventional and subspace based algorithms to estimate Direction of Arrival (DOA)[C]// 2016 International Conference on Communication and Signal Processing (ICCSP). IEEE, 2016.
5. N. S. John, A. G. Konstantinos, S. Katherine. On the Direction of Arrival (DOA) Estimation for a Switched-Beam Antenna System Using Neural Networks[J]. IEEE Transactions on Antennas and Propagation, 2009, 57(5):1399-1411.
6. X. Wu, W. P. Zhu, J. Yan. A High-Resolution DOA Estimation Method With a Family of Nonconvex Penalties[J]. IEEE Transactions on Vehicular Technology, 2017, pp (99).
7. Y. Bin, H. Feng, J. Jin, et al. DOA estimation for attitude determination on communication satellites[J]. Chinese Journal of Aeronautics, 2014, 27(3): 670-677.
8. O. Alamu, B. Iyaomolere, A. Abdulrahman. An overview of massive MIMO localization techniques in wireless cellular networks: Recent advances and outlook[J]. Ad Hoc Networks, 2021, 111:102353.

9. P. Ponnusamy, K. Subramaniam, S. Chintagunta. Computationally efficient method for joint DOD and DOA estimation of coherent targets in MIMO radar[J]. Signal processing, 2019, 165(Dec.):262-267.
10. E. Baidoo, J. Hu, B. Zeng, et al. Joint DOD and DOA estimation using tensor reconstruction based sparse representation approach for bistatic MIMO radar with unknown noise effect[J]. Signal Processing, 2020, 182(Dec. (12)):107912.
11. X. Wang, W. Wang, J. Liu, et al. A sparse representation scheme for angle estimation in monostatic MIMO radar[J]. Signal Processing, 2014, 104:258-263.
12. B. Yao, Z. Dong, W. Liu. Effective joint DOA-DOD estimation for the coexistence of uncorrelated and coherent signals in massive multi-input multi-output array systems[J]. EURASIP J. Adv. Signal Process. 2018, 64 (2018).
13. X. Wang, M. Huang, L. Wan. Joint 2D-DOD and 2D-DOA Estimation for Coprime EMVS–MIMO Radar[J]. Circuits Systems and Signal Processing, 2021:1-17.
14. R. Schmidt. Multiple emitter location and signal parameter estimation, IEEE Transactions on Antennas and Propagation, March 1986, vol. 34, no. 3, pp. 276-280.
15. Y. Hu, T. D. Abhayapala, P. N. Samarasinghe. Multiple Source Direction of Arrival Estimations Using Relative Sound Pressure Based MUSIC[J]. IEEE/ACM Transactions on Audio, Speech, and Language Processing, 2020, 29(99):1-1.
16. R. Roy, T. Kailath. ESPRIT-estimation of signal parameters via rotational invariance techniques[J], IEEE Transactions on Acoustics, Speech, and Signal Processing, July 1989, vol. 37, no. 7, pp. 984-995.
17. Y. Jung, H. Jeon, S. Lee, et al. Scalable ESPRIT Processor for Direction-of-Arrival Estimation of Frequency Modulated Continuous Wave Radar[J]. Electronics, 2021, 10(6):695.
18. Q. Si, Y. D. Zhang, M. G. Amin. Generalized Coprime Array Configurations for Direction-of-Arrival Estimation[J]. IEEE Transactions on Signal Processing, 2015, 63(6):1377-1390.
19. P. Pal, P. P. Vaidyanathan. Nested Arrays: A Novel Approach to Array Processing with Enhanced Degrees of Freedom[J]. IEEE Transactions on Signal Processing, 2010, 58(8):4167-4181.
20. Y. Pang, S. Liu, Y. He. A PE-MUSIC Algorithm for Sparse Array in MIMO Radar[J]. Mathematical Problems in Engineering, 2021, 2021.
21. M. C. Hucumenoglu, P. Pal. Effect of Sparse Array Geometry on Estimation of Co-array Signal Subspace[C]// 2020 International Applied Computational Electromagnetics Society Symposium (ACES). IEEE, 2020.
22. A. Beulahv, N. Venkateswaran. Sparse linear array in the estimation of AOA and AOD with high resolution and low complexity[J]. Transactions on Emerging Telecommunications Technologies, 2019.
23. P. P. Vaidyanathan, P. Pal. Sparse Sensing with Co-Prime Samplers and Arrays[J]. IEEE Transactions on Signal Processing, 2011, 59(2):573 - 586.
24. C. Zhou, Z. Shi, Y. Gu, et al. DECOM: DOA estimation with combined MUSIC for coprime array[C]// International Conference on Wireless Communications & Signal Processing. IEEE, 2013.

25. P. Pal, P. P. Vaidyanathan. Coprime sampling and the MUSIC algorithm[C]// Digital Signal Processing Workshop and IEEE Signal Processing Education Workshop (DSP/SPE), IEEE, 2011.
26. J. Li, D. Jiang, X. Zhang. DOA Estimation Based on Combined Unitary ESPRIT for Coprime MIMO Radar[J]. IEEE Communications Letters, 2017, 21(1):96-99.
27. J. Li, X. Zhang, D. Jiang. DOD and DOA estimation for bistatic coprime MIMO radar based on combined ESPRIT. Cie International Conference on Radar IEEE, 2016.
28. W. Zhou, Q. Wang, J. Tang. DOA estimation of MIMO radar with unistatic expansion coprime array[J]. Journal of Nanjing University of Posts and Telecommunications: Natural Science Edition, 2019(6):1-8.
29. C. Adnet, P. Gounon, J. Galy. High Resolution Array Processing for Non circular Signals[C]// Signal Processing Conference. IEEE, 2010.
30. K. Gowri, P. Palanisamy, I. S. Amiri. Improved Method of Direction Finding for Non circular Signals with Wavelet Denoising Using Three Parallel Uniform Linear Arrays[J]. Wireless Personal Communications, 2020(4).

Figures

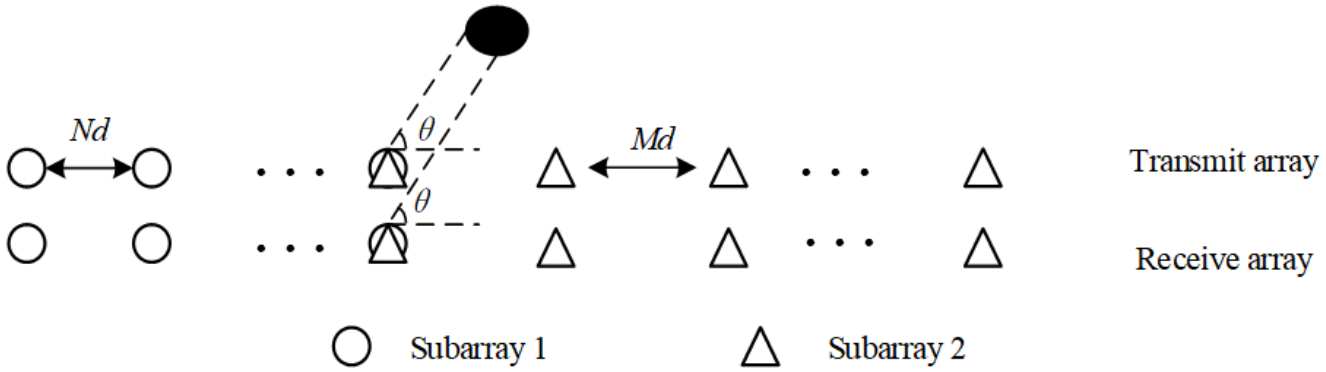

Figure 1

Coprime MIMO radar array geometry

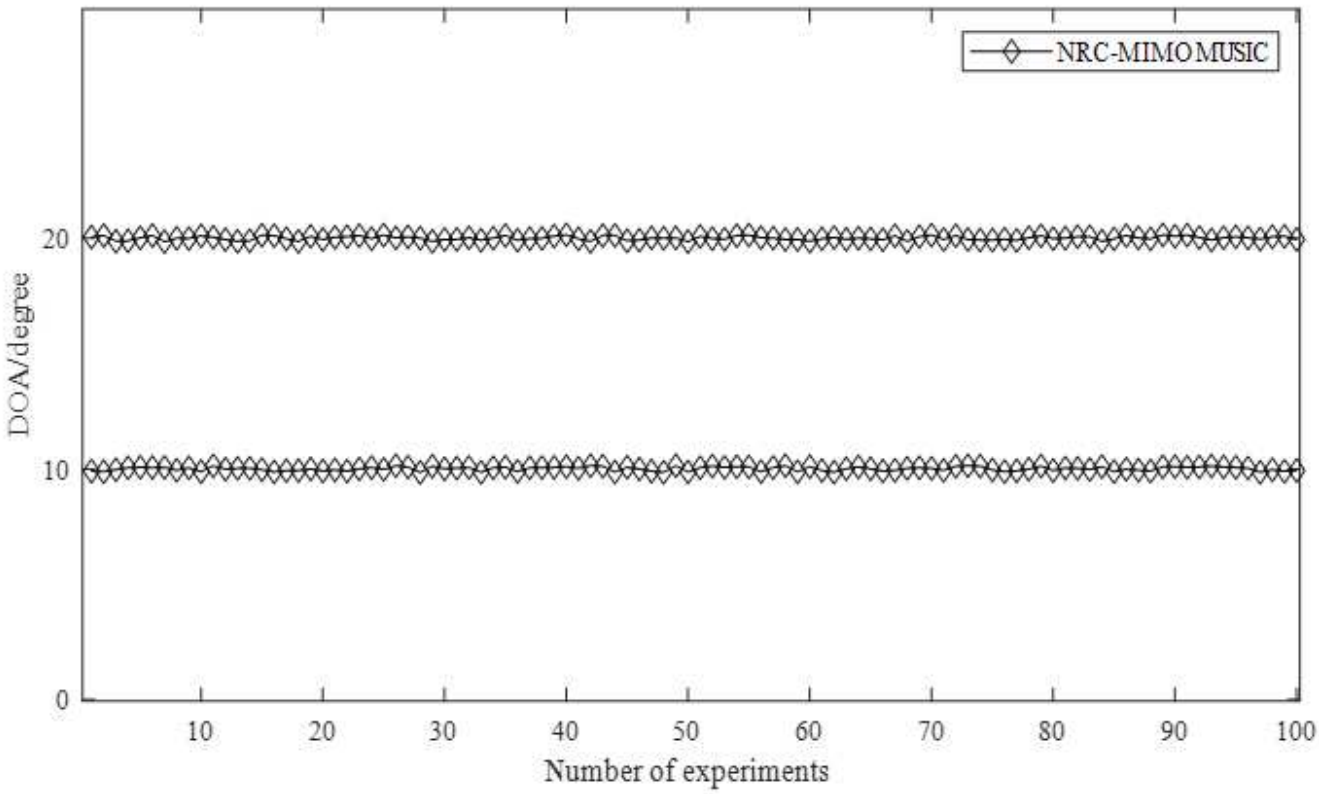

Figure 2

Algorithm estimation performance under SNR=10 dB

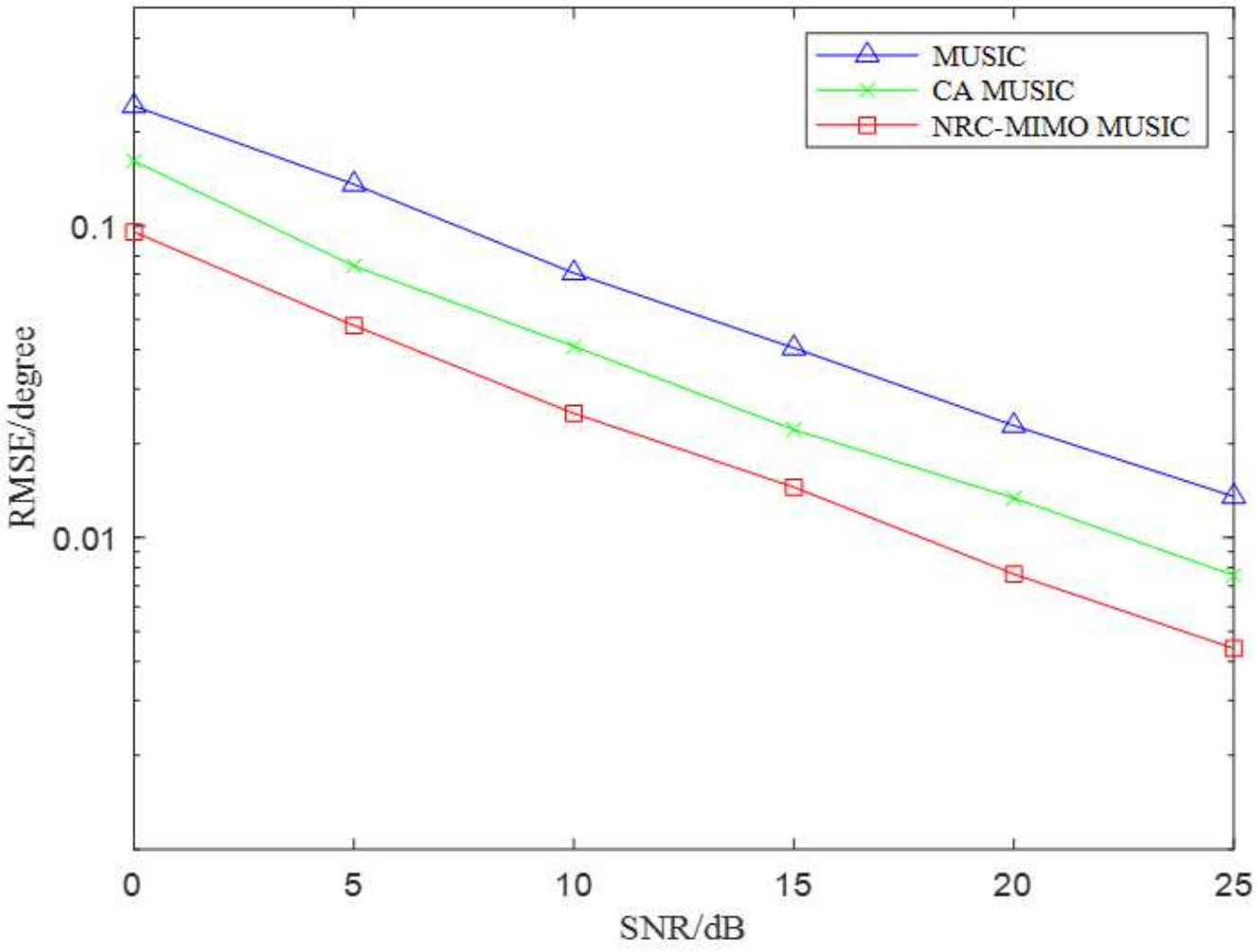

Figure 3

Estimation performance changes under different SNR

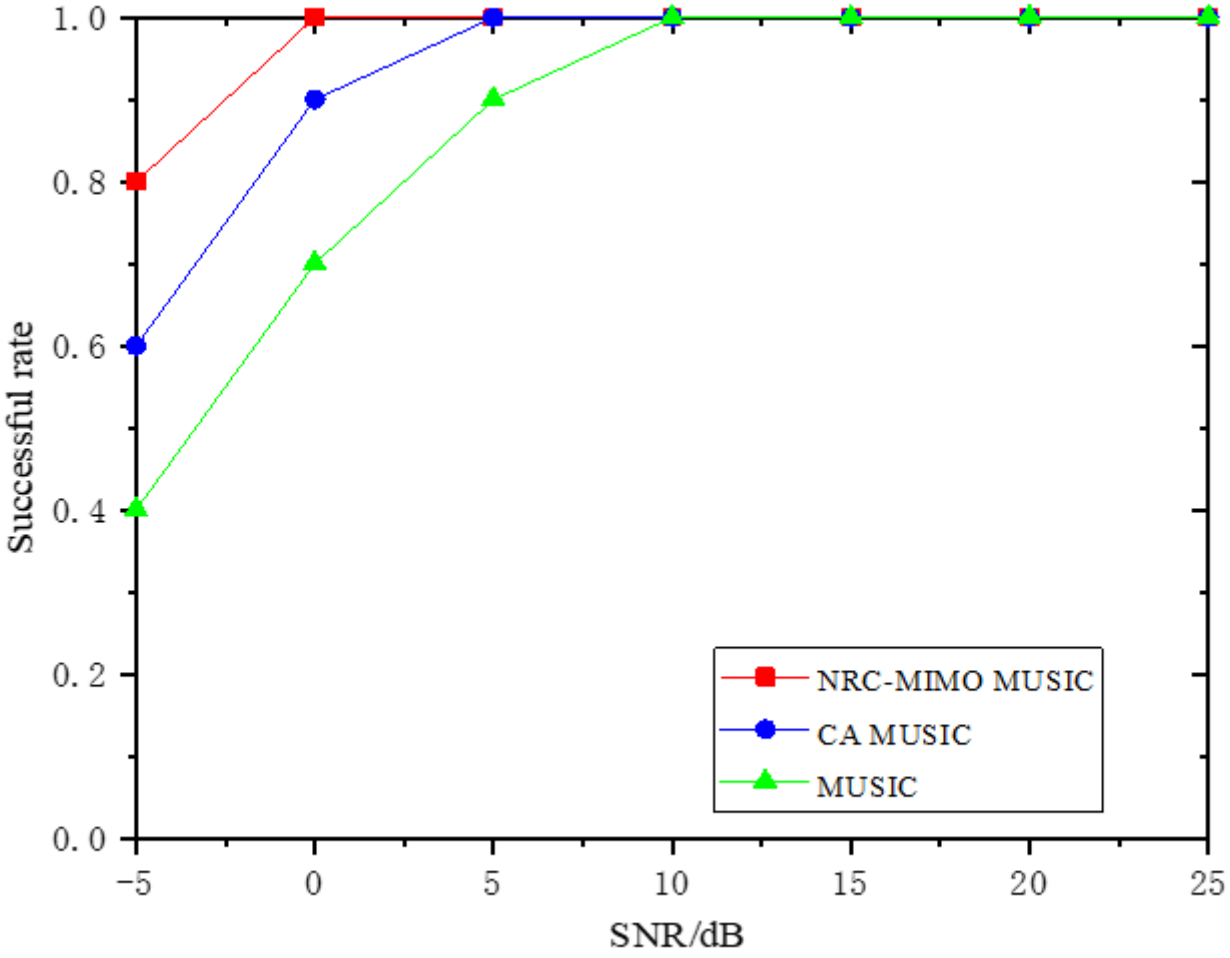

Figure 4

The target detection success rate varies with SNR

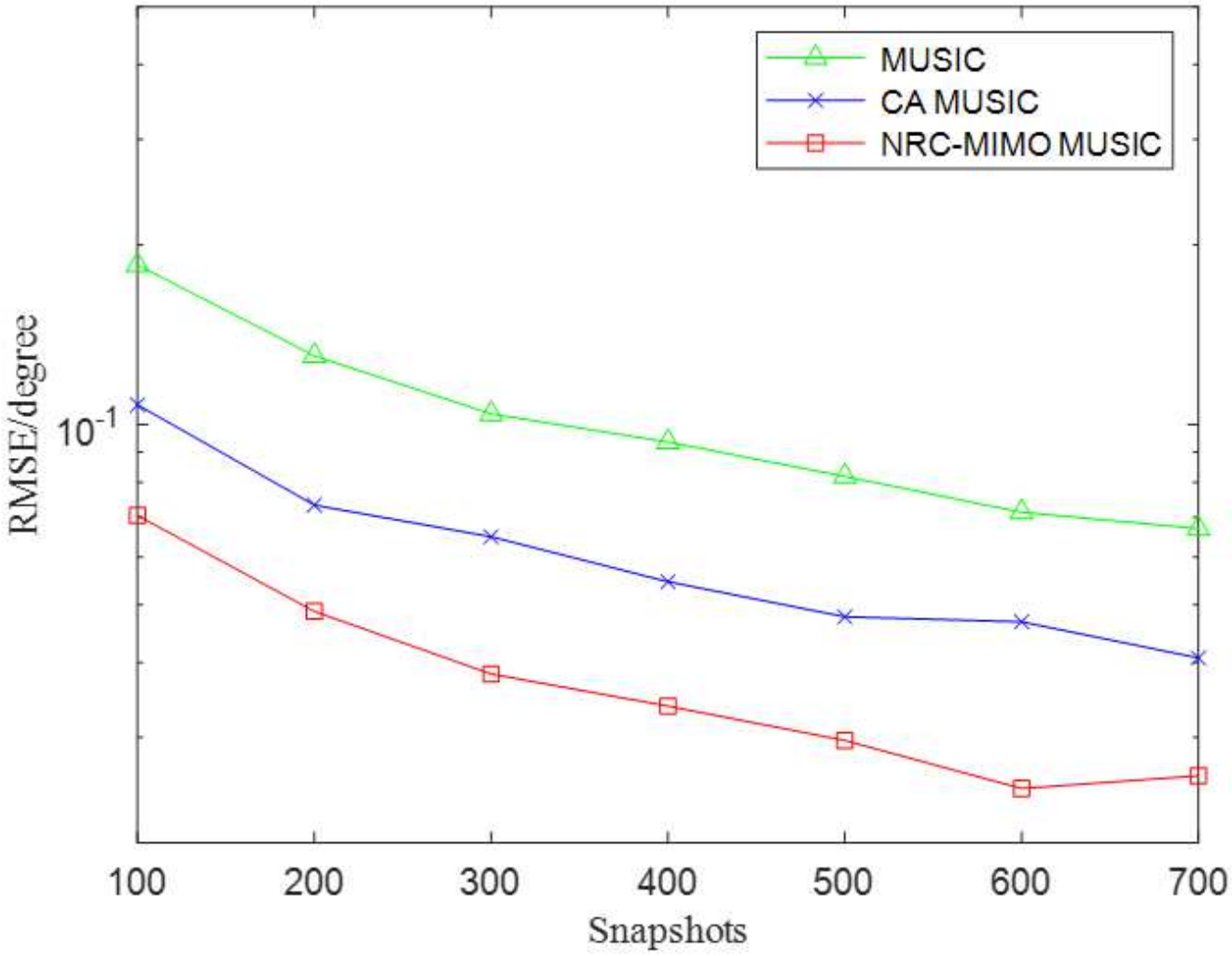

Figure 5

Estimated performance changes under different snapshots

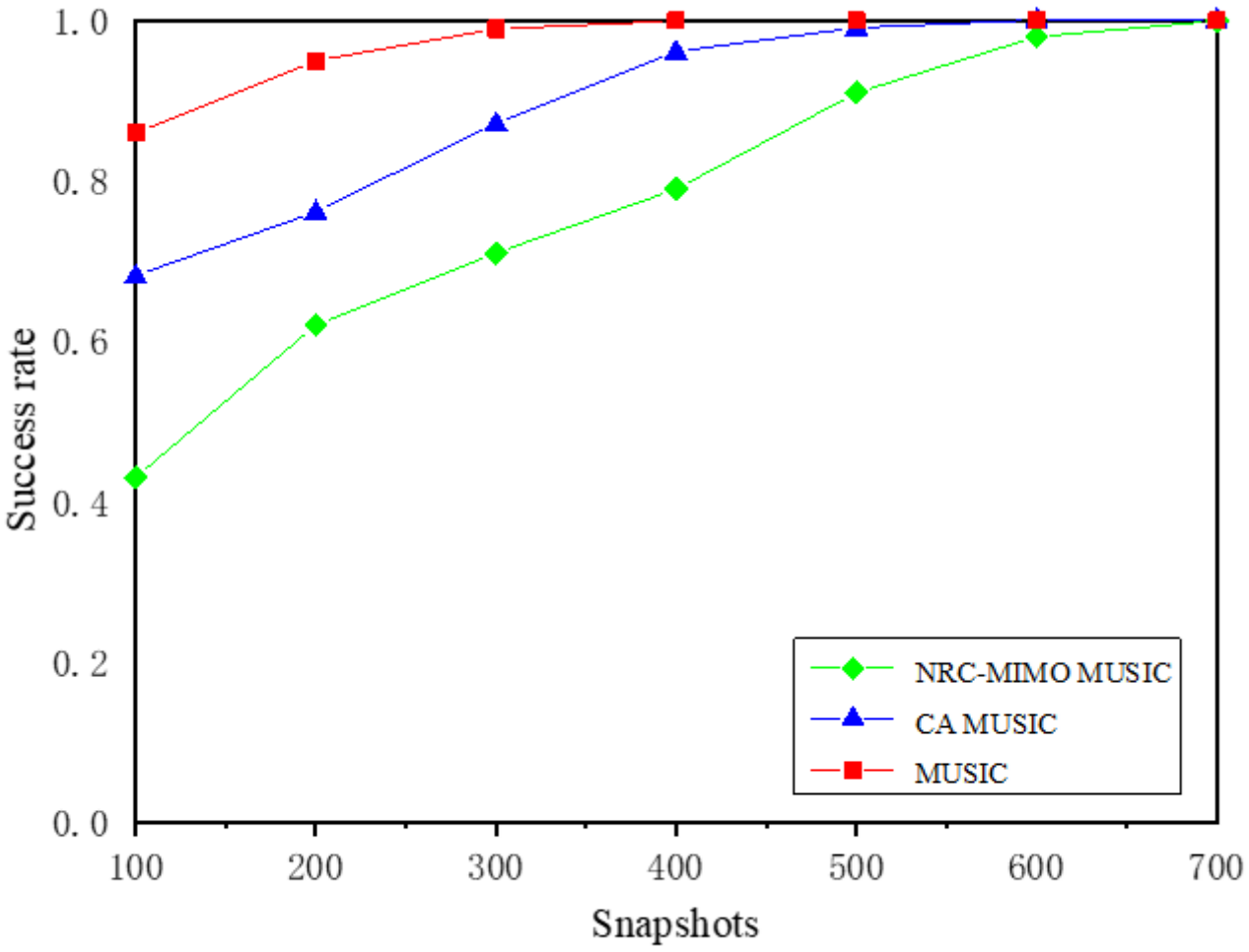

Figure 6

The success rate of target detection varies with the number of snapshots

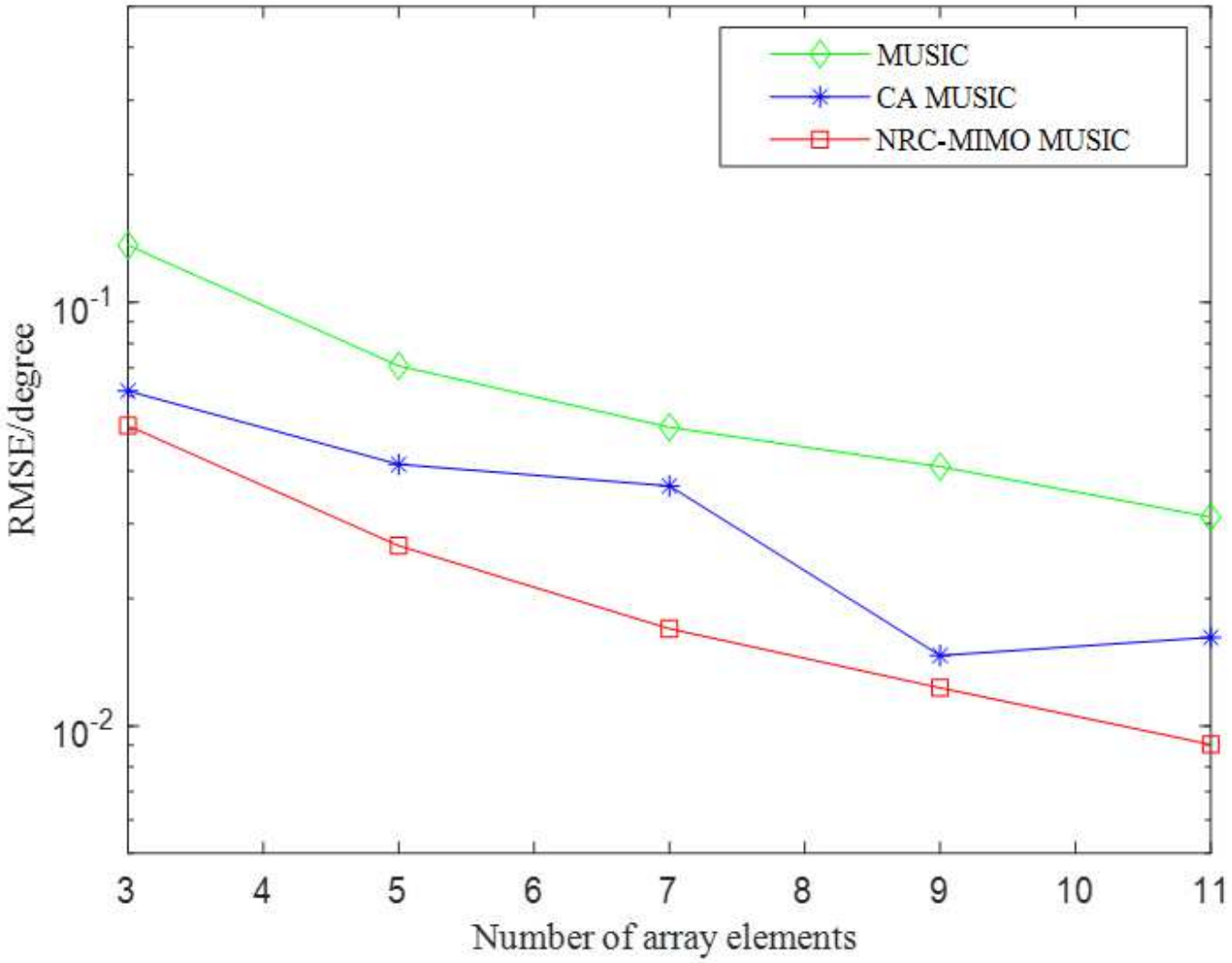

Figure 7

Relationship between the estimation accuracy and the number of array elements

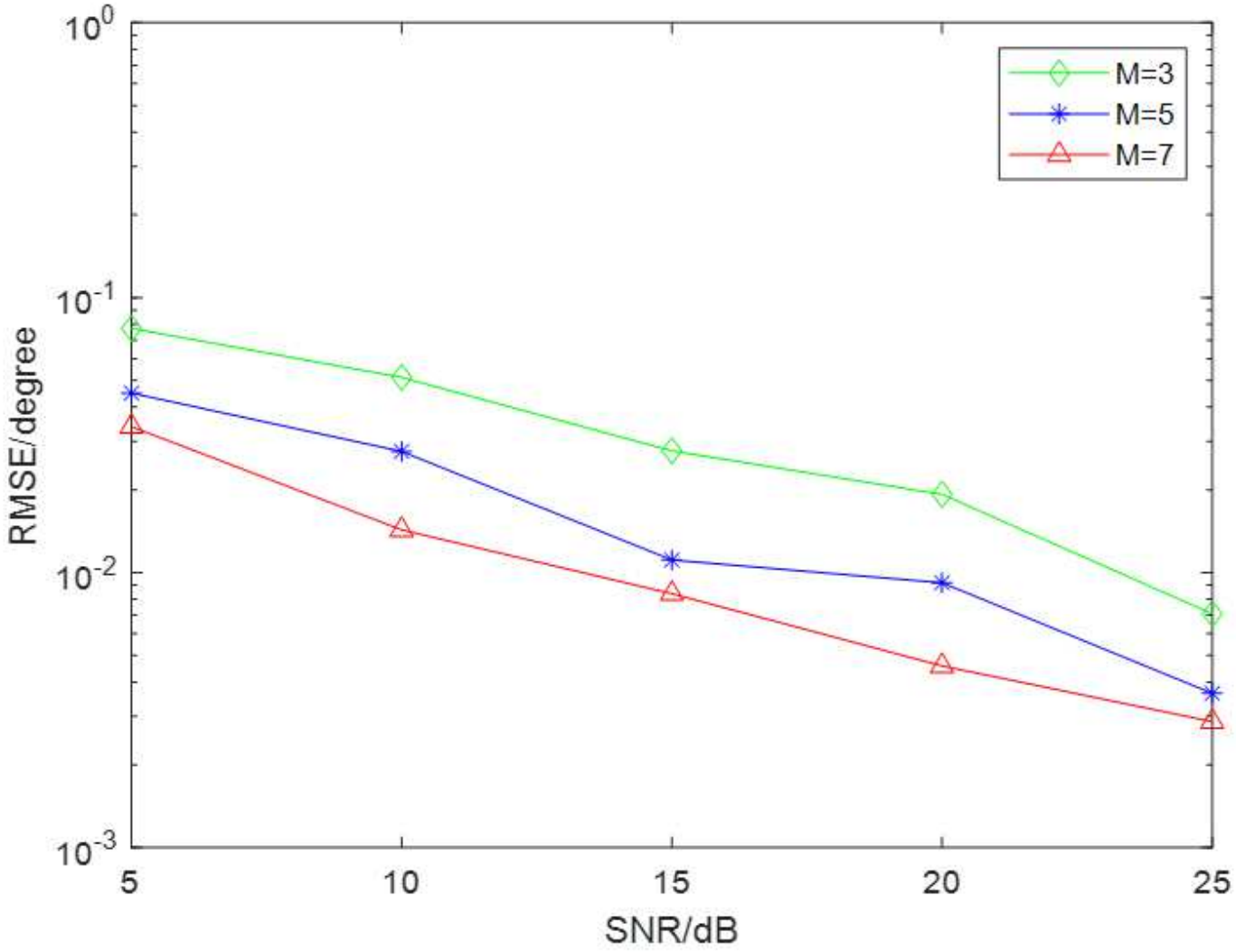

Figure 8

Performance comparison of algorithms with different numbers of transmitting array elements